Optimization of a 250-GHz Schottky Tripler Using Novel Fabrication and Design Techniques

John Thornton, Chris M. Mann, and Peter de Maagt, *Member, IEEE*

***Abstract*—A technique for optimizing a diode waveguide mount for millimeter- and submillimeter-wave applications has been developed. The structure consists of a planar rectangular radiator for which an accurate derivation of impedance is available. The planar radiating probe incorporates the diode contacting tip, is fabricated integrally with the microstrip filter, and is used in a 230–290-GHz frequency tripler. Modification of the tripler using the described technique resulted in an improvement of ≈6 dB in available output power, compared to the authors' previous results for this device. Device output power exceeds 8.5 mW at 245 GHz for an input power of 132 mW. The best flange-to-flange efficiency (in excess of 11%) was achieved at 3.3–mW output power. This technique was then applied to a waveguide mount, incorporating two diodes contacted in parallel, so that greater input power could be handled. This resulted in a tripler with a maximum output power of 15 mW at 270 GHz for an input of 280 mW.**

***Index Terms*—Frequency multiplication, millimeter-wave frequency converters, Schottky diode frequency converters, varactor.**

I. Introduction

In THE drive to realize solid-state heterodyne mixers for space applications at frequencies above 1 THz, the provision of sufficient local oscillator (LO) power is a critical issue. To realize the LO from solid-state sources, cascaded frequency multiplier stages are a practical solution. Substantial power has been reported from solid-state LO chains around 300 GHz (up to 8 mW) [1], [2], and similar levels could be expected at 400 GHz in the near future—a final tripler stage with an efficiency of ≈6% could provide sufficient power at 1.25 THz to drive a subharmonic mixer at 2.5 THz (a key frequency for atmospheric research).

In addition, there are serious moves toward complete device integration via micromachined waveguide [3] and, in order for this approach to be successful, accurate modeling of the waveguide circuit prior to fabrication will be essential since empirical optimization will be difficult.

An approach is described where lithographic techniques are used to fabricate a planar waveguide radiating probe for which a fast accurate analytical model is available. This is a simple, but important step. Previously, the wire whiskers used in many millimeter- and submillimeter-wave circuits had to perform both electrical and mechanical roles. In order to make a mechanically stable contact to the diode, the whisker would require some form of bend, which complicated the electrical analysis—as reliability is often the driving factor, the electrical performance would inevitably be sacrificed to the mechanical requirements.

However, a lithographically produced "planar" whisker may take any two-dimensional shape. Because the planar whisker's natural springiness keeps the contacting tip in place, there is no need for an additional bend. Therefore, the whisker's shape can be "fitted" to the analytical model without approximations being made. In addition, the approach will also be useful for matching planar diodes in waveguide by considering the metallization of the diode chip.

Manuscript received September 11, 1996; revised May 11, 1998. This work was supported in part by the European Space Agency under Contract 153770.

J. Thornton is with the Department of Engineering Science, University of Oxford, Oxford, Oxon. 0X1 3PJ, U.K.

C. M. Mann is with the Millimetre Wave Technology Group, Rutherford Appleton Laboratory (RAL), Chilton, Oxon. OX11 0QX, U.K.

P. de Maagt is with the European Space Research and Technology Centre (ESTEC), European Space Agency, Noordwijk, The Netherlands.

Publisher Item Identifier S 0018-9480(98)05516-1.

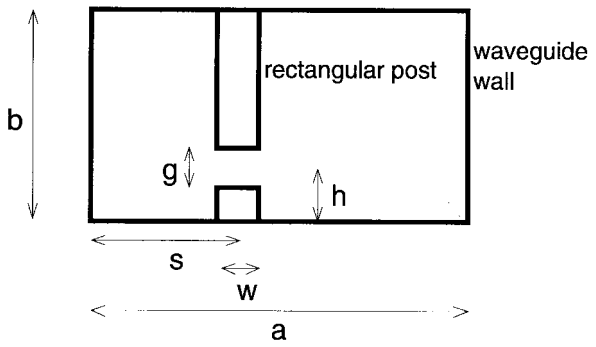

Fig. 1. Waveguide and post dimensions (after [4]).

II. Determination of Probe Inductance

An analytical method [4] for the driving impedance of a gap in a rectangular strip across a waveguide of rectangular cross section was used as the basis for matching the diode to the waveguide in a frequency tripler. The geometry is shown in Fig. 1.

The impedance is effectively a function of the coupling between the currents in the post and an infinite series of waveguide modes which may exist. The analysis derives an expression for gap impedance consisting of a double summation for all possible waveguide modes. In practice, it is only necessary to consider a finite number of modes with no significant loss of accuracy.

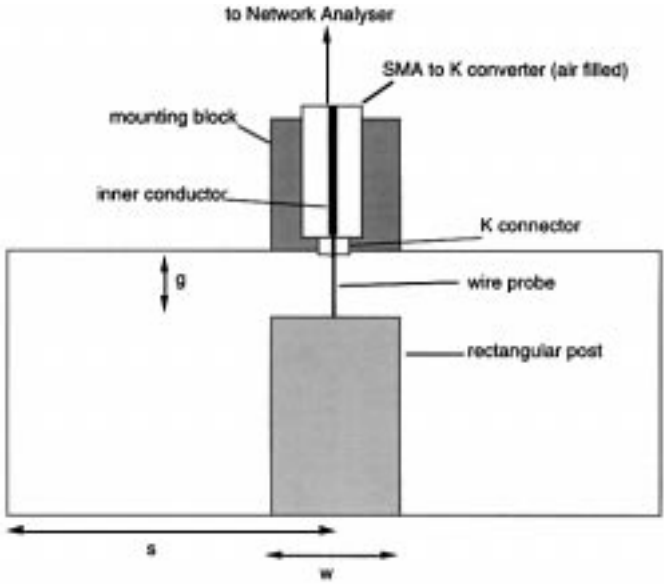

Fig. 2. Waveguide model in cross section showing schematic of measurement system.

The two waveguide arms can each be terminated by any complex reflection coefficient. This is particularly useful when considering devices such as multipliers, where different harmonics of the pump frequency are terminated in different ways.

Practical verification of the analysis was performed with measurements made on a low-frequency scale model of the rectangular post in the instance where it spans the entire waveguide apart from a gap between the end of the post and waveguide wall. A microstrip filter channel was not included. A measurement technique was devised which utilized a Wiltron K-connector between the coaxial measurement line and a 200-μm-diameter wire probe spanning the gap between the waveguide wall and rectangular post. This allowed the plane of calibration to be moved as close as possible to the point of measurement. The model and measurement system is represented in Fig. 2.

Since the dimensions of the K-connector (outer diameter 0.45 mm) are small compared to the waveguide cross section (40.4 mm $\times$ 10.0 mm) the discontinuity introduced by the connector itself is minimal—in fact, the scaled dimensions of the connector are similar to those of a typical varactor diode anode used around 300 GHz. A Hewlett-Packard 8510B vector network analyzer was used over a 2–12-GHz frequency range.

The impedance measured at the aperture of the K-connector is essentially the same as what a diode would experience if placed at this position. In order to relate the impedance calculated from [4] to the impedance measured in the model, the parallel inductance of the wire measurement probe placed across the gap between the waveguide wall and the end of the rectangular post must be found. This effect is taken into account of (in [4]) by the introduction of an equivalent circuit. However, when this circuit was tried in our model for a large number of cases with varying post size and gap width, it gave conflicting results. In order to obtain good agreement between the measured and computed results, it was necessary to manually adjust the individual values of the circuit elements. The aim of this work was to provide a complete model for the probe, including the whisker tip (wire measurement probe). Therefore, to provide a more general solution, it was decided to derive an empirical expression which would provide the values for the equivalent-circuit elements for all post/probe configurations.

Many measurements were made for different values of post width w and gap size g. In each case, the measured and computed results were "fitted" by introducing an appropriate value for the wire probe's inductance in the computed result. This had the effect of moving the predicted data around in a clockwise direction on the Smith chart until it aligned with the measured results. Using this procedure, an empirical model for the wire probe inductance as a function of w and g was determined. For our measurement configuration, the capacitance used in the equivalent circuit of [4] was found to have a negligible effect. The most obvious reason for this is that in the configuration analyzed in [4], the flat strip was approximated to a cylindrical post by setting the equivalent width w of the cylindrical post to $w = 1.8d$ where d is the diameter of the post (no such approximation is necessary for this paper). For a cylindrical post, the capacitance between its end and the waveguide wall would be considerably higher than that for the flat post used here, and would thus require an additional capacitance to the equivalent circuit in order to take this into account.

A. Model for the Inductance of the Wire Measurement Probe

The wire measurement probe inductance L is expected to have two physical components, which are: the discontinuity between the narrow wire measurement probe and the wider rectangular post (L_{dis}) and the series inductance of the wire measurement probe (L_{ser}). For each case of post width w, the data L versus g was fitted to a least-squares fit for a straight line. The y-axis intercept is interpreted as the discontinuity inductance and the slope of the line as L_{ser}/g for the series inductance.

L_{dis} was seen to increase with w—a linear fit gave

$$L_{\text{dis}} = 0.015w \text{ nH}, \qquad \text{where } w \text{ is in mm.} \tag{1}$$

L_{ser}/g was also seen to increase with w. This is expected since the series inductance of a packaged diode whisker is often approximated by the inductance of a coaxial line

$$L_{\text{coax}} = \frac{\mu l \log[b/a]}{2\pi} \tag{2}$$

where μ is permeability of medium, l is length of line, and a and b are radii of inner and outer coaxial conductors, respectively.

In our geometry, the magnetic field around the probe is confined to a region related to dimension w [5]. For these reasons, the results for L_{ser}/g versus w were fitted to a logarithmic function, where

$$L_{\text{ser}}/g = \log[1.247 + (0.0944(w-1)) - (0.002(w-1)^2)]. \tag{3}$$

Fig. 3 shows the logarithmic fit and experimental data.

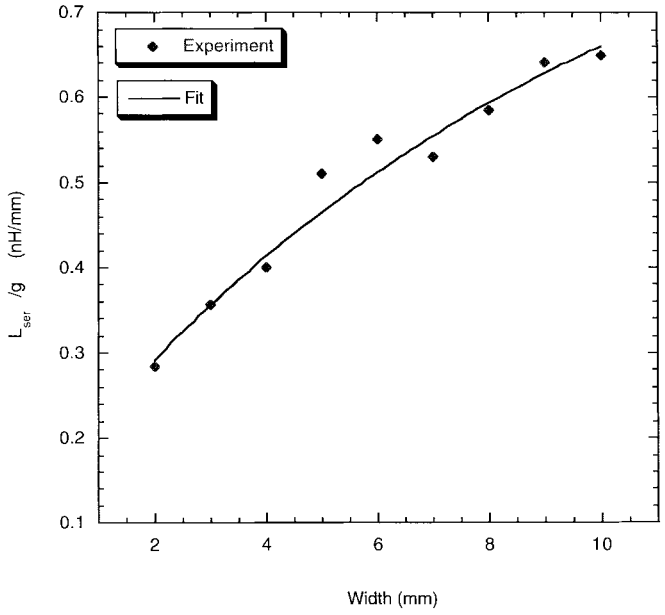

Fig. 3. Logarithmic fit for $L_{\rm ser}/g$.

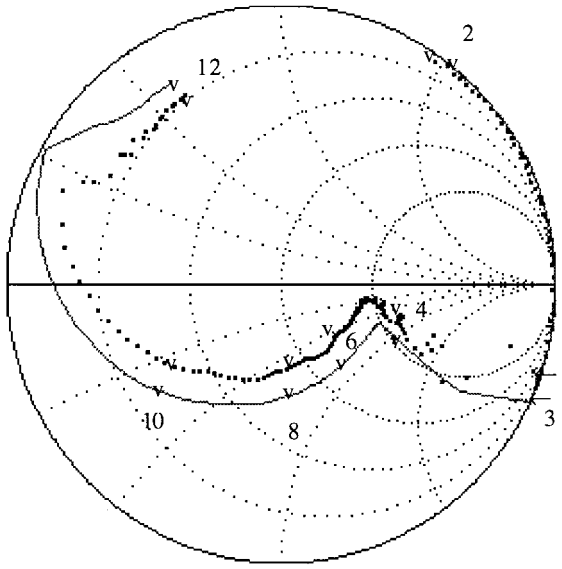

Fig. 4. Example of theoretical and experimental results for combined impedance of post and measurement probe.

By combining (1) and (3), we have the following complete empirically derived expression for L as a function of w and g:

$$L = 0.015w + g\log[1.247 + (0.0944(w-1)) - (0.002(w-1)^2)]\ \text{nH},$$

where w and g are given in mm. (4)

This expression may then be used to derive an approximate value for the inductance of the whisker contacting tip, which takes the place of the wire measurement probe in the actual Schottky diode device.

Typical results from the waveguide model, where the waveguide arms are terminated in matched loads, are presented in Fig. 4 and show a level of agreement between computed and measured results which gave the authors a high degree of confidence in the approach taken. In each case, the post was centrally located in the waveguide to emulate the geometry of the tripler. For the example shown (see Fig. 4), $w = 8.0$ mm and $g = 1.35$ mm. Over 60 variations of post width and gap have been tried and, in all cases, similar or better levels of agreement were obtained. Plots showing these results can be found in [6].

III. Application of Techniques to the Development of a Frequency Multiplier

With the accuracy of the analysis now verified and extended to include an empirical model for the wire measurement probe (or whisker tip) inductance, it was used to modify the design of an existing frequency tripler with a nominal operating range of 230–290 GHz. This tripler when assembled using conventional wire-whisker techniques by the authors had not previously been seen to exceed 2.5-mW output power at saturation. The design of this tripler had been based closely on that of an established crossed waveguide geometry [7].

A strength of the analysis [4] is that any complex reflection coefficient for each waveguide arm may be included. Thus, the short circuit presented by the tuner and the second harmonic idler were included in the computer program.

TABLE I
Optimum Embedding Impedances for a Frequency-Tripling Varactor Diode at Selected Operating Frequencies

harmonic	optimum impedance (Ω).		
	at 250 GHz	at 270 GHz.	at 290 GHz
1st.	120 + j 300	105 + j 275	84 + j 256
2nd.	0 + j 175	0 + j 158	0 + j 155
3rd.	53 + j 108	48 + j 98	44 + j 92

The optimum embedding impedances for a University of Virginia type-5M4 varactor diode at the first three harmonic frequencies were derived using a harmonic-balance program [8]. The diode parameters salient to the harmonic-balance program are

$$C_0 = 1.5 \times 10^{-14}\ \text{F}$$
$$\gamma = 0.5$$
$$I_s = 2.7 \times 10^{-17}\ \text{A}$$
$$\phi = 1.0\ \text{V}$$

where C_0 is the zero-bias capacitance, I_s is the zero-bias leakage current, ϕ is the inherent barrier potential, and the doping factor $\gamma = 0.5$ represents an abrupt junction with nongraded doping.

Series resistance R_s was measured to be $8.0 \pm 0.5\ \Omega$, ideality η was measured to be 1.08

An input power of 50 mW was assumed and three output frequencies (250, 270, and 290 GHz) were studied—the optimum impedance at each harmonic was found to vary little over this frequency range, as can be seen in Table I.

By using the computer model, it was possible to derive rectangular post dimensions (width w and gap size g) which would provide the optimum impedance for the third harmonic

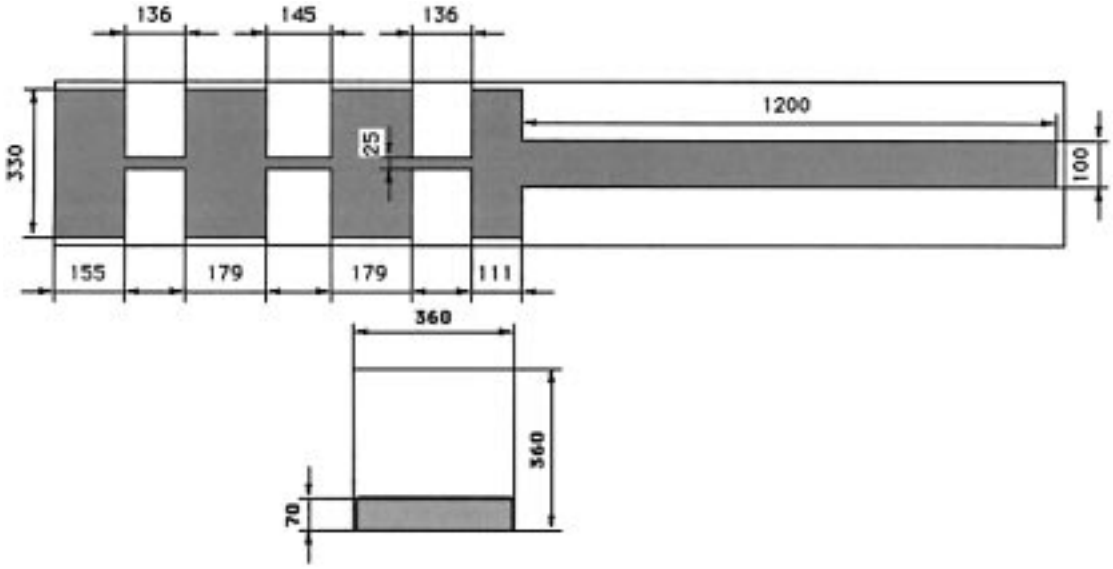

Fig. 5. Schematic diagram of the box microstrip filter design with an end view of the filter cavity (all dimensions in microns).

at a particular tuner position. Peak power output may then be expected for a tuner position where the second harmonic embedding impedance (reactive) and third harmonic embedding impedance (complex) are both close to the optimum condition. The fundamental or pump frequency input circuit is independently tunable, allowing it to be treated as a separate problem. A high-power carcinotron was employed as the pump signal source and output power was measured using both an Anritsu power head (manufacturer calibrated) and Keating power meter, which were in agreement to $\pm 10\%$.

IV. Tripler Performance

Having chosen the post dimensions w and g, an integrated planar post and whisker structure was fabricated photolithographically. The whisker tip length corresponded to the gap size g. It was also possible to produce an integral structure, which included a microstrip radio-frequency (RF) filter. The filter was designed to provide a phase that was as close to a short circuit at the waveguide wall as possible for the second, third, and fourth harmonics, so as to comply with the Eisenhart and Khan analysis. For an earlier design where the filter deviated substantially from this condition, these phase variations were observed to have an effect on the device's behavior [9]. For this same reason, the diode was buried into the whisker post so that electrically it appears to form part of the waveguide wall. The seven-section microstrip filter design is shown in Fig. 5 with the filter cavity enclosure. The fused quartz substrate was 70-μm-thick, and 2-μm-thick gold metallization was used for the filter circuit and planar whisker probe.

Fabrication of the planar whisker structure is very straightforward, and a detailed description is given in [10]. A 75-mm-diameter 0.5-mm-thick fused quartz wafer is used as the base substrate material. This is coated in 2-μm-thick gold and to aid adhesion, a 50-nm-thick layer of nichrome is used as an interface layer. Conventional wet processing is used to pattern the outline of the filters integrated with the planar whisker contacting probes. The unwanted quartz is then removed using a combination of mechanical lapping and chemical etching.

The substrate is mounted metallization side down onto a silicon-wafer carrier using Stronghold wax[1] which melts at 100 °C and readily dissolves in acetone at room temperature. Care must be taken to ensure that the filter/planar whiskers are in intimate contact with the surface of the silicon wafer and that both are level. The silicon carrier is then mounted onto the table of a dicing saw, and a wide blade ($\approx$0.25 mm) is used to machine the unwanted quartz away. The blade is stepped in the horizontal plane in $\approx$0.25-mm increments, removing $\approx$100 μm per tranverse. This process is repeated until the thickness of quartz remaining behind the filters is $\approx$120 μm. A thinner blade is then used to create a trench directly behind the whiskers. Approximately 15 μm of quartz is left intact behind the whiskers, although the exact thickness is not important. The complete wafer is now immersed in buffered hydrofluoric acid to remove the quartz directly behind the whiskers. Then, the substrate is returned to the dicing saw for backlapping to the correct thickness and filter separation. Finally, the exposed nichrome is removed, and the individual filters/whisker substrates washed from the silicon carrier using acetone.

A contacted RF structure spanning the output waveguide is shown in Fig. 6. The diode anode face is flush with the waveguide wall opposite to the filter. The waveguide width is 1.1 mm, height is 0.229 mm, the probe is 0.115-mm-wide, and the contacting tip is 30-μm-long.

To examine the validity of this approach—i.e., designing a structure which presents the optimum impedance derived from a harmonic-balance program—the predicted power over the whole range of backshort tuner movement was derived by calculating the embedding impedance at the second, third, and fourth harmonics at small increments of tuner position. The embedding impedance at the pump frequency (which is independently tunable) was assumed to be a constant value

[1] J. H. Young Company Inc., Rochester, NY 14611.

Fig. 6. Assembled and contacted tripler circuit.

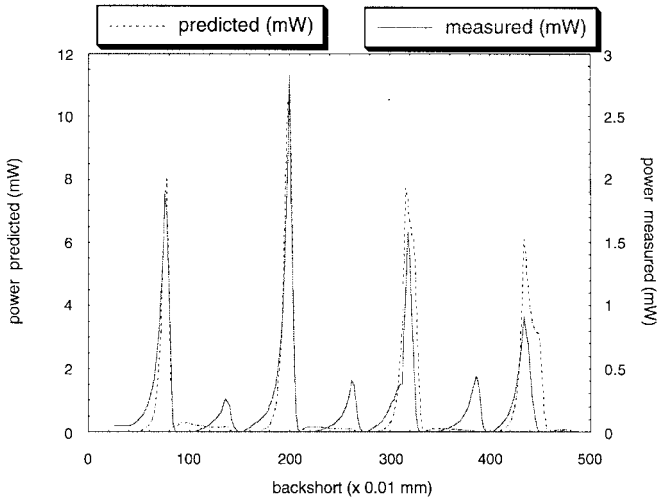

Fig. 7. Calculated and measured output power as a function of backshort position (at 274-GHz and 40-mW input power).

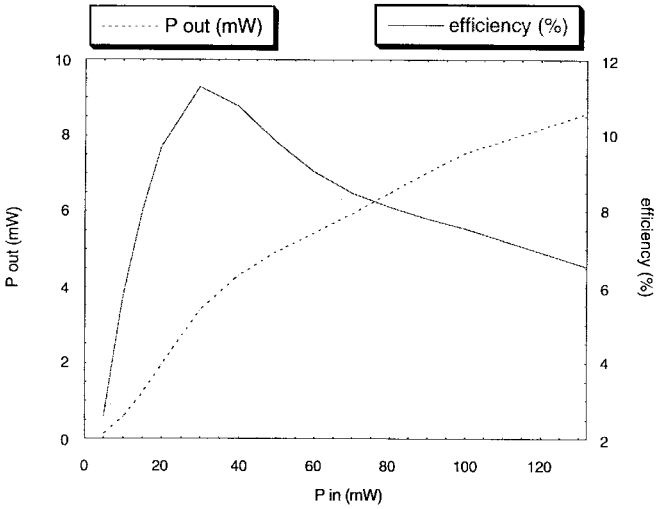

Fig. 8. Measured power and efficiency versus input power (at 245 GHz).

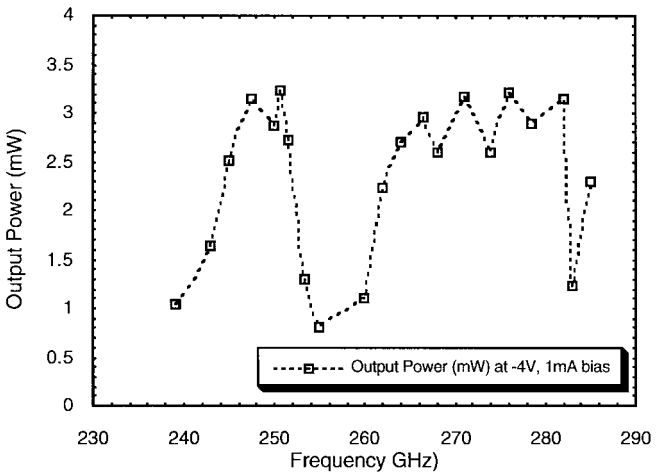

Fig. 9. Measured tripler power output versus frequency (input power 30 mW).

close to the optimum. By using these impedance values in the harmonic-balance program, the power output was predicted at each position and compared with the measured output of the device, as shown in Fig. 7 (where the input power is limited to 40 mW.)

In Fig. 7, the level of agreement in the shape of the two curves demonstrates the potential of the combined analysis, particularly in identifying the backshort position required for peak output power and predicting the envelope of the amplitude of the major peaks, which is set by the relative phase between the second, third, and fourth harmonics. The measured output power is inevitably lower than the predicted power since losses in the input and output waveguides, LO filter, and waveguide tuners are not accounted for by the harmonic-balance program. Also, the poor agreement of the minor peaks suggests that an unknown phase change is occurring in the mount, e.g., the idler termination for the second harmonic or, as described later (see Section VI), within the diode itself.

The maximum measured output power was observed at a frequency of 245 GHz. The efficiency and output power at this frequency are shown as a function of input power in Fig. 8.

A maximum output power of 8.6 mW corresponded to an input power of 132 mW at 6-V reverse bias and a forward current of 3 mA. When driven more conservatively, a 3.3-mW output power corresponded to 11% flange-to-flange efficiency. To the author's knowledge, this represents the highest reported output power to date obtained from a Schottky varactor tripler at these frequencies. One notable exception of 11 mW obtained at 225 GHz [11] was reported for a device where the varactor diode had been biased well into the reverse breakdown region, leading it to subsequent burn out after a short period of time. The tripler reported here was used for tens of hours before finally being dismantled and reassembled, as discussed in the Section V.

The device works over a broad frequency range, as can be seen from Fig. 9, but there is an adverse resonance in the central-frequency region. Because this feature is common to three separate triplers constructed using different filters and probes, it is likely that this resonance is due to some

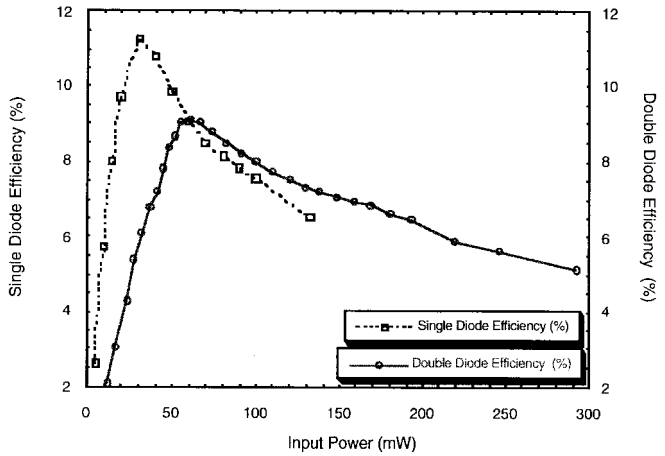

(a)

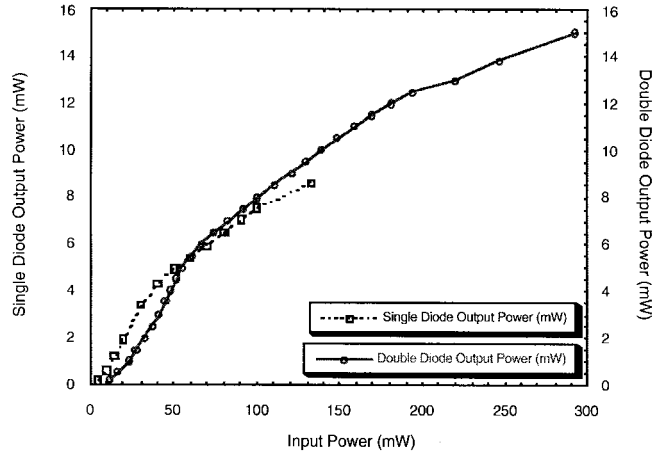

(b)

Fig. 10. (a) Efficiencies and (b) power outputs for the single- and double-diode multipliers.

characteristic of the waveguide idler circuit (the one common feature of all three devices). Removing this resonance should yield further gains in efficiency and output power.

V. Application to Higher Output Powers

To further increase the output power of the device, two diode anodes were contacted in parallel using a planar whisker that had two tips placed very close to one another. This increases the effective anode area by a factor of two and, hence, doubles the overall capacitance, and increases the input power which may be used. The peak efficiency is then expected to occur for a correspondingly greater input power than the single diode case.

To determine what embedding impedance is optimum for such a diode pair, the harmonic-balance code was rerun for a single diode of twice the area. Using the technique described above, a probe was designed to provide this impedance. The tripler was reassembled using this probe and tested. The results were highly encouraging—an output power of 15 mW at 270 GHz was obtained, at an input power level of 280 mW.

Fig. 10 shows the measured efficiency and output powers for both the single- and double-diode case. The lower peak efficiency seen for the two-diode case is attributed to not providing the optimum embedding impedance to the two diodes. Their representation as a single diode of twice the area is probably an oversimplification and further empirical optimization might yield additional improvement in performance. Nevertheless, to our knowledge, this is the highest reported output power from a tripler at 270 GHz.

VI. Conclusions

This paper has demonstrated the validity of a model used for predicting the impedance presented by a planar radiating structure to a varactor diode in waveguide and has been applied to the development of a powerful millimeter-wave source. The approach has given insight into the mode of operation of a millimeter-wave multiplier and has been useful in identifying deficiencies in the device, which are now being addressed.

Since the diode whisker contacting structure that has been developed is planar in nature, the method may be readily extended to the use of planar diode chips and is, therefore, highly applicable to the optimization of millimeter-wave waveguide mixers, subharmonic mixers, doublers, and higher order multipliers. Also, because the circuit is fabricated lithographically and is very straightforward to assemble, the technique is readily scaleable to terahertz frequencies.

Interestingly, recent work [12] which used embedding impedances derived from the method described above in conjunction with a more complete model for the diode (one that addresses electron transport phenomena at these frequencies), has highlighted differences when compared to the conventional equivalent-circuit model [8]. In particular, this approach [12] was able to predict the minor peaks that appear in Fig. 7, which the diode equivalent-circuit model used in this paper could not.

Acknowledgment

The authors would like to express thanks to all members of the Rutherfors Appleton Laboratory (RAL), Millimeter Wave Technology Group, Oxon., U.K., and microwave workshop, without whose help this work would not have been possible.

References

[1] P. Zimmermann, "Frequency multipliers and LO sources for the submillimeter wave region," presented at the Proc. ESA Workshop Millimeter Wave Tech. Appl. ESTEC, Noordwijk, The Netherlands, Dec. 1995.

[2] P. J. Koh, W. C. B. Peatman, T. W. Crowe, and N. R. Erickson, "Novel planar varactor diodes," presented at the 7th Int. Symp. Space THz Technol., Charlottesville, NC, Mar. 1996.

[3] D. A. Brown, A. S. Treen, and N. J. Cronin, "Micromachining of terahertz waveguide components with integrated active devices," presented at the 19th Int. Conf. Infrared Millimeter Waves, Sendai, Japan, 1994.

[4] R. L. Eisenhart and P. J. Khan, "Theoretical and experimental analysis of a waveguide mounting structure," *IEEE Trans. Microwave Theory Tech.*, vol. MTT-19, pp. 706–719, Aug. 1971.

[5] W. J. Getsinger, "The packaged and mounted diode as a microwave circuit," *IEEE Trans. Microwave Theory Tech.*, vol. MTT-14, pp. 58–69, Feb. 1966.

[6] J. Thornton, "An analytical model for a rectangular antenna in a metallic enclosure and its use for the optimization of a 250GHz source for antenna characterization," ESA, European Space Research and Technology Centre (ESTEC), Noordwijk, The Netherlands, Final Rep., 1996.

[7] J. W. Archer, "An efficient 200–290 GHz frequency tripler incorporating a novel stripline structure," *IEEE Trans. Microwave Theory Tech.*, vol. MTT-32, pp. 416–420, Apr. 1984.

[8] P. H. Siegel, A. R. Kerr, and W. Hwang, "Topics in the optimization of millimeter wave mixers," NASA, Washington, DC, Tech. Paper 2287, Mar. 1984.
[9] J. Thornton and C. M. Mann, "A design approach for planar waveguide launching structures," presented at the 7th Int. Symp. Space Terahertz Technol., Univ. Virginia, Mar. 1996.
[10] C. M. Mann, "A novel 183 GHz subharmonic Schottky diode mixer," Ph.D. dissertation, Queen Mary and Westfield College, Univ. London, London, U.K., pp. 210–211, 1991.
[11] N. R. Erickson, "Very high efficiency frequency triplers for 100–300 GHz," in *IEEE Int. Conf. Submillimeter Waves Applicat.*, 1985, pp. 54–55.
[12] R. E. Lipsey, C. Mann, S. H. Jones, and J. Thornton, "The complete analysis of a 91.33 to 275 GHz Schottky barrier varactor frequency tripler," presented at the 8th Int. Symp. Space Terahertz Technol., Boston, MA, Mar. 1997.

John Thornton was born in Lancs., U.K., in 1968. He received the B.Sc. degree in physics from the University of York, York, U.K., in 1989, and the M.Sc. degree from the University of Portsmouth, Portsmouth, U.K., in 1995.

From 1995 to 1997, he worked with the Millimeter Wave Technology Group, Rutherford Appleton Laboratory (RAL), Oxon., U.K., where he specialized in the development of solid-state frequency multipliers for spaceborne receivers from 200 to 500 GHz. The group recorded increasing LO power levels during this period, which lead to the successful realization of solid-state unbiased subharmonic receivers at 500 and 560 GHz. He is currently with the Department of Engineering Science, University of Oxford, Oxon., U.K., where his more recent research activities have involved the development of novel modulated microwave reflectors, which operate as passive transponders at commercial radar frequencies (this technique has been pioneered at Oxford).

Chris M. Mann was born in London, U.K., in 1962. He received the B.Sc. degree with honours from Coventry Poletechnic, Lanchester, U.K., in 1985, and the Ph.D. degree from the University of London, London, U.K., in 1992.

From 1985 to 1992, he was an Associate Researcher at the Rutherford Appleton Laboratory (RAL), Oxon., U.K., where he worked on numerous aspects of millimeter-wave technology, including superconductor/insulator/superconductor (SIS) junction fabrication, space hardware, and a novel 183-GHz subharmonic mixer. In 1992, he joined the Photodynamics Research Centre, Sendai, Japan, where he was involved with the design of corner cube mixers at 1.4 THz and the use of analytical models for the prediction of waveguide-circuit embedding impedance. In 1994, he returned to RAL, playing a leading role in the design, fabrication, and testing of the world's first 2.5-THz waveguide mixer in 1995. Since then, he has continued this work, but is also working on the optimization of submillimeter-wave frequency multipliers and subharmonic mixers and is currently pioneering waveguide micromachining techniques in order to realize completely integrated submillimeter-wave RF frontends.

Peter de Maagt (S'88–M'88) was born in Pauluspolder, The Netherlands, in 1964. He received the M.Sc. and Ph.D. degrees from Eindhoven University of Technology, Eindhoven, The Netherlands, in 1988 and 1992, respectively, both in electrical engineering.

He is currently with the European Space Research and Technology Centre (ESTEC), European Space Agency, Noordwijk, The Netherlands. His research interests are in the area of millimeter- and submillimeter-wave reflector and planar integrated antennas, quasi-optics, photonic bandgap antennas, and millimeter- and submillimeter-wave components.